

# A transient method for total emissivity estimation

B Zhang, J Redgrove, J Clark

*Centre for Basic, Thermal and Length Metrology, National Physical Laboratory,  
Queens Road, Teddington, Middlesex, TW11 0LW, UK  
Email: [bufa.zhang@npl.co.uk](mailto:bufa.zhang@npl.co.uk)*

## **Abstract**

A transient method for determining the total emissivity of solids is presented using the emissometer recently developed at the NPL. Emissivity is calculated from measurement of the sample surface temperature coupled with knowledge of its bulk thermal properties. This was conducted as part of the present validation of the new NPL apparatus for high temperature emissivity measurements.

Theoretical study shows that the sample surface temperature depends solely on total emissivity and effusivity when a thermally thick sample is radiating freely to a cold environment. Total emissivity measurements made on FeCrAlloy steel are presented to investigate the feasibility of the proposed method for total emissivity estimation.

## **1 Introduction**

Hemispherical total emissivity is a thermal radiative property of materials that is particularly important in engineering at high temperatures. Conventional techniques for measuring hemispherical total emissivity include the direct-heating method where a dc current is allowed to pass through a metallic sample and emissivity is determined from the measured sample surface temperature, area and electrical power lost by radiation from its surface [Touloukian and DeWitt, 1970]. For non-metallic materials that cannot be self-heated, emissivity can be calculated by integrating angular spectral emissivity values measured using a radiometric method [Touloukian and DeWitt, 1972]. Use of the Fourier transform spectrometer (FTS) makes total emissivity evaluation much easier and more accurate since an FTS can measure radiation over a wide range of wavelengths with high spectral resolution [Ballico and Jones, 1995; Werner, 1995/1996; Clausen *et al*, 1996]. Measurements at angles to the sample surface need to be performed for calculating the hemispherical total emissivity of the sample.

A main source of uncertainty in steady-state emissivity measurement methods is due to surface temperature measurement. To overcome this difficulty, a transient technique has been developed at NPL [Redgrove, 1985] in which the sample is first heated to a steady, uniform temperature in a furnace and a plane surface of the sample is then rapidly exposed to a cold environment and begins to radiate freely, during which time its thermal spectral radiation signal is measured and recorded. To reduce the measurement uncertainty caused by the limited exposure speed, the recorded transient data are fitted to a theoretical model to allow extrapolation of the data back to time 'zero',

corresponding to the initial isothermal condition. This allows accurate determination of target radiation at the initial isothermal temperature and thus, following comparison with a blackbody measurement, an accurate sample emissivity value.

A new NPL emissometer has been developed recently which uses a Fourier transform spectrometer to widen the ranges of temperature and wavelength, and allows well-defined angular measurements at angles up to  $70^\circ$  to the sample surface using a periscope [Zhang *et al*, 2002]. Therefore, hemispherical total emissivity can be calculated by integrating angular spectral emissivity values.

The work presented here was conducted as part of validating the new apparatus for high temperature emissivity measurement. The aim was to determine hemispherical total emissivity by monitoring sample surface temperature and apply the theoretical solution for a freely radiating semi-infinite solid and then compare with the total emissivity value obtained independently by integration of angular spectral emissivity measurements.

## 2 Method

During a transient emissivity measurement in vacuum heat is lost from the sample surface by thermal radiation. If the sample is assumed to be homogeneous, isotropic, optically opaque and thermally wide and thick enough, it can be considered as a semi-infinite solid for modelling purposes. Also, assuming that emissivity is unchanged during the measurement – on the basis that emissivity is usually a weak function of temperature and the temperature change during measurement is only a few or few 10s of degrees – then the changing sample surface temperature can be calculated from the measured radiation signal.

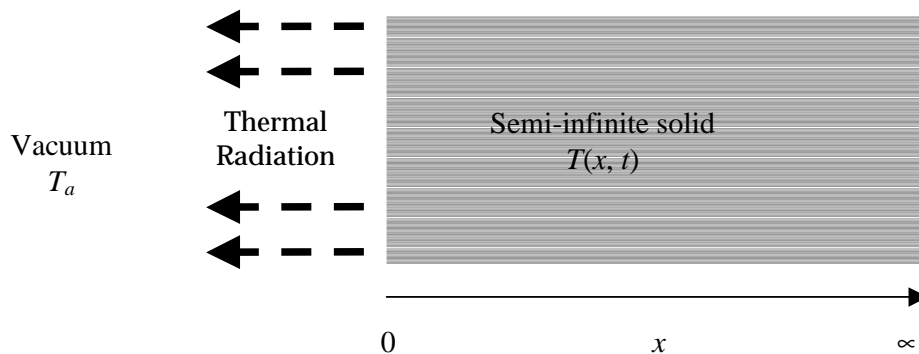


Figure 1 Semi-infinite solid sample radiating into a vacuum at temperature  $T_a$ .

The surface temperature of a semi-infinite sample with surface radiation cooling has been investigated by Jaeger [1950] and this forms the basis of the method we have adopted here for estimation of total emissivity. Taking a co-ordinate system as shown in figure 1, the temperature field,  $T(x, t)$ , inside the sample can be described by Fourier's equation as

$$\frac{\partial^2 T}{\partial x^2} = \frac{1}{\alpha} \frac{\partial T}{\partial t} \quad (1)$$

where  $\alpha$  is the thermal diffusivity of the sample, together with the initial condition:

$$T(x, 0) = T_0 \quad (2)$$

for  $x \geq 0$  and  $T_0$  is the initial ( $t = 0$ ) temperature of the sample, and the radiation heat flux  $q(t)$  at the surface ( $x = 0$ ) is

$$q(t) = \varepsilon \sigma (T_s^4 - T_a^4) \quad (3)$$

for a grey sample, where

$$T_s(t) = T(0, t) \quad (4)$$

is the temperature at the sample surface.  $T_a$  is the temperature of the environment to which the sample surface is radiating freely,  $\varepsilon$  is the hemispherical total emissivity of the sample surface and  $\sigma = 5.67 \cdot 10^{-8} \text{ Wm}^{-2}\text{K}^{-4}$  the Stefan-Boltzmann constant. For continuity of heat flow at the sample surface, the following condition also applies

$$q(t) = \kappa \frac{\partial T}{\partial x} \quad (5)$$

where  $\kappa$  is the thermal conductivity of the sample. The exact solution for equation (1) with the conditions of equations (2) and (3) can be calculated [Jaeger, 1950] and the surface temperature  $T_s(t)$  is given by (see Appendix):

$$T_s(t) = T_0 \left[ 1 + \sum_{n=1}^{\infty} \frac{a_n}{n!} \left( \frac{t}{t_0} \right)^{\frac{n}{2}} \right] \quad (6)$$

for  $t > 0$ , where

$$t_0 = \frac{p^2}{\varepsilon^2 \sigma^2 T_0^6} \quad (7)$$

is a specific time related to the sample thermal properties and initial sample temperature,  $T_0$ .  $p = \sqrt{\kappa \rho C_p}$  is the effusivity of the material and,  $\rho$  and  $C_p$  are the density and specific heat capacity respectively, linking thermal conductivity  $\kappa$  and diffusivity  $\alpha$  by  $\kappa = \alpha \rho C_p$ . The term  $a_n$  is the  $n^{\text{th}}$  coefficient, which becomes constant

when the initial sample temperature  $T_0$  is much higher than the temperature of its environment  $T_a$  as discussed in the Appendix. Equation (6) shows that the decrease in surface temperature is thus solely dependent on  $t/t_0$ .

Once surface temperature has been calculated, equation (3) can be used to evaluate the thermal radiative heat flux at the sample surface, which can be expressed in the form of a Taylor series as follows:

$$q(t) = q_0 \left[ 1 + \sum_{n=1}^{\infty} \frac{b_n}{n!} \left( \frac{t}{t_0} \right)^{\frac{n}{2}} \right] - \frac{T_a^4}{T_0^4} q_0 \quad (8)$$

for  $t > 0$ , where  $q_0 = \varepsilon \sigma T_0^4$  and  $b_n$  is the  $n^{\text{th}}$  coefficient given in the Appendix. Using Planck's law and equation (6), the spectral radiation signal at wavelength  $\lambda$  is given by:

$$S(\lambda, t) = S_0(\lambda) \frac{e^{\frac{C_2}{\lambda T_0}} - 1}{e^{\frac{C_2}{\lambda T_s}} - 1} \quad (9)$$

for  $t > 0$ , where  $S_0(\lambda)$  is the initial spectral radiation signal at wavelength  $\lambda$ , including the instrument factor of the apparatus, and  $C_2 = 14388 \mu\text{m K}$  is the second radiation constant. For the purpose of curve-fitting to measurement data, using equation (6) for  $T_s$  and expanding equation (9) as a Taylor series in  $(t/t_0)^{1/2}$  (see Appendix), gives:

$$S(\lambda, t) = S_0(\lambda) \left[ 1 + \sum_{n=1}^{\infty} \frac{d_n}{n!} \left( \frac{t}{t_0} \right)^{\frac{n}{2}} \right] \quad (10)$$

where  $d_n$  is the  $n^{\text{th}}$  coefficient, a function of  $T_a/T_0$  and  $\lambda T_0$ . Equation (10) shows that the decrease in spectral radiation signal is dependent on  $t/t_0$  and the parameters  $T_a/T_0$  and  $\lambda T_0$ .

Calculations have been performed to evaluate the changes with time of the sample surface temperature, heat flux and spectral radiation signals. Equations (6), (8) and (10) show that, when normalised by their initial values at  $t = 0$ , those quantities can be presented using a dimensionless time scale,  $t/t_0$ , and thereby become independent of the sample thermal properties.

For small values of time  $t$ , the series in equations (6), (8) and (10) are rapidly convergent and only a few of the  $a_n$ ,  $b_n$  and  $d_n$  values need to be computed. For example, for  $t < 0.01t_0$ , the computation error due to taking only the first two  $a_n$  values is less than 1.2%, and less than 0.53% error with three  $a_n$  values, less than 0.33% with four  $a_n$  values and so on. The effect on sample surface temperature caused by the measurement environment being at temperatures above 0 K are considered below.

(a) **Surface temperature:** Figure 2 shows surface temperature calculations where the initial temperature of the sample varies between 400 K and 1000 K, and the environment temperatures are 0 K and 300 K respectively. It can be seen that the surface temperature decreases less rapidly when the sample surface is exposed to a 300 K environment than to a 0 K one. This is because the sample surface absorbs some radiation from the environment, at least when  $T_a > 0$  K. It is noticed that environment temperature has a significant effect on changes in sample surface temperature when it is not much lower than the sample temperature (*e.g.*  $T_0 = 400$  K in figure 2). However, this effect becomes negligibly small when the temperature difference between sample and environment is large (*e.g.*  $T_0 = 1000$  K to  $T_a = 300$  K in figure 2).

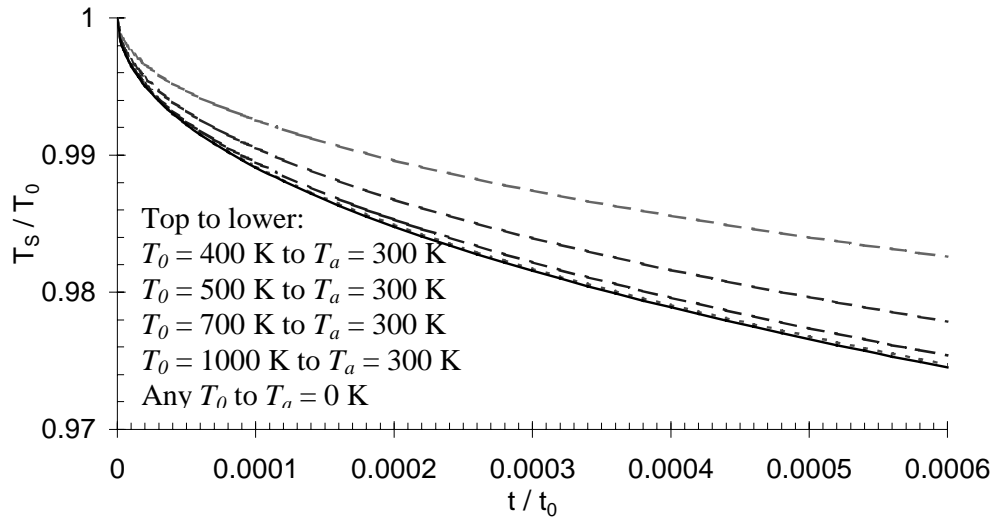


Figure 2 Calculations of sample surface temperature v. time for radiation from the surface into an environment at 300 K (dashed lines) and 0 K (solid line).

(b) **Surface radiative heat flux:** Figure 3 shows that net heat flux from the sample can depend strongly on the difference between the sample and environment temperatures. For example, when the temperature of the sample is 400 K the flux is 30% less for  $T_a = 300$  K than when  $T_a = 0$  K. The flux difference decreases as the temperature difference between sample and environment increases.

(c) **Spectral radiation signal:** Spectral radiation signals are calculated in figure 4 to show that the spectral radiation signals change with time in a similar way to that for the surface temperature, but at much greater rates. The signals depend on environment temperature and, more significantly, on wavelength.

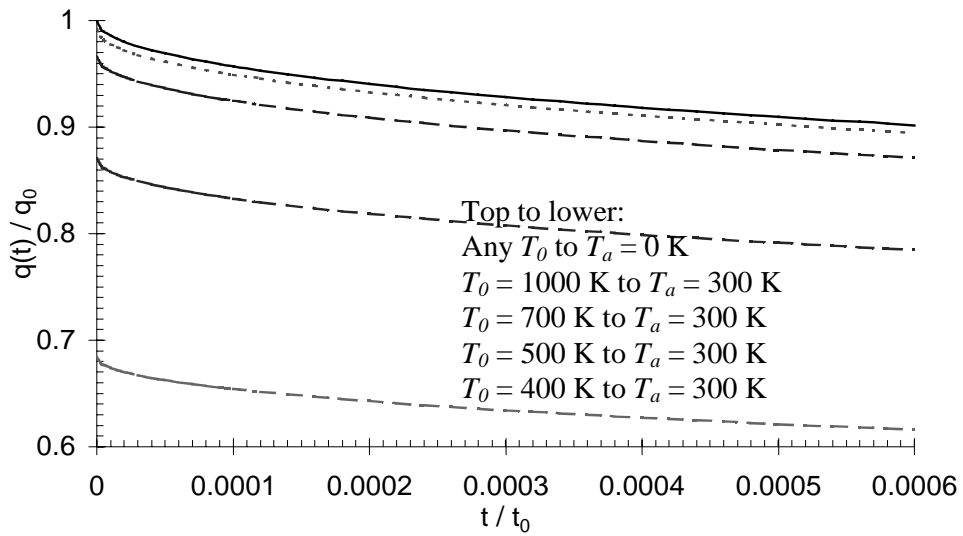


Figure 3 Calculation of radiative heat flux v. time.

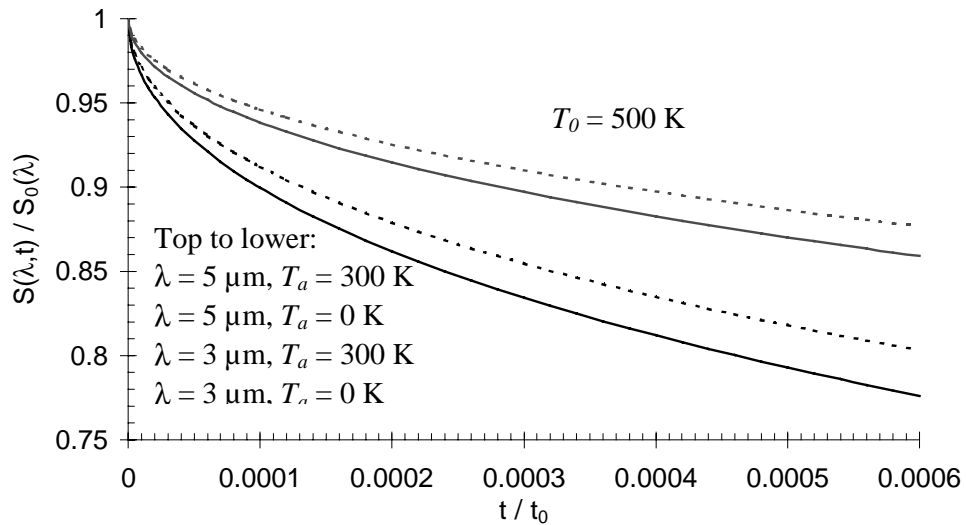


Figure 4 Calculation of spectral radiation signal v. time.

### 3 Apparatus

Figure 5 shows the new NPL apparatus. A computer controls the shutter motor and performs data analysis on signals acquired from the FT spectrometer. The FTS measures radiation from the sample or blackbody cavity obtained via the vacuum chamber periscope and CaF<sub>2</sub> window. Within the vacuum chamber are four main parts: a

movable tantalum heating furnace, graphite sample block, high-speed shutter and periscope for viewing the detected area at a well-defined angle.

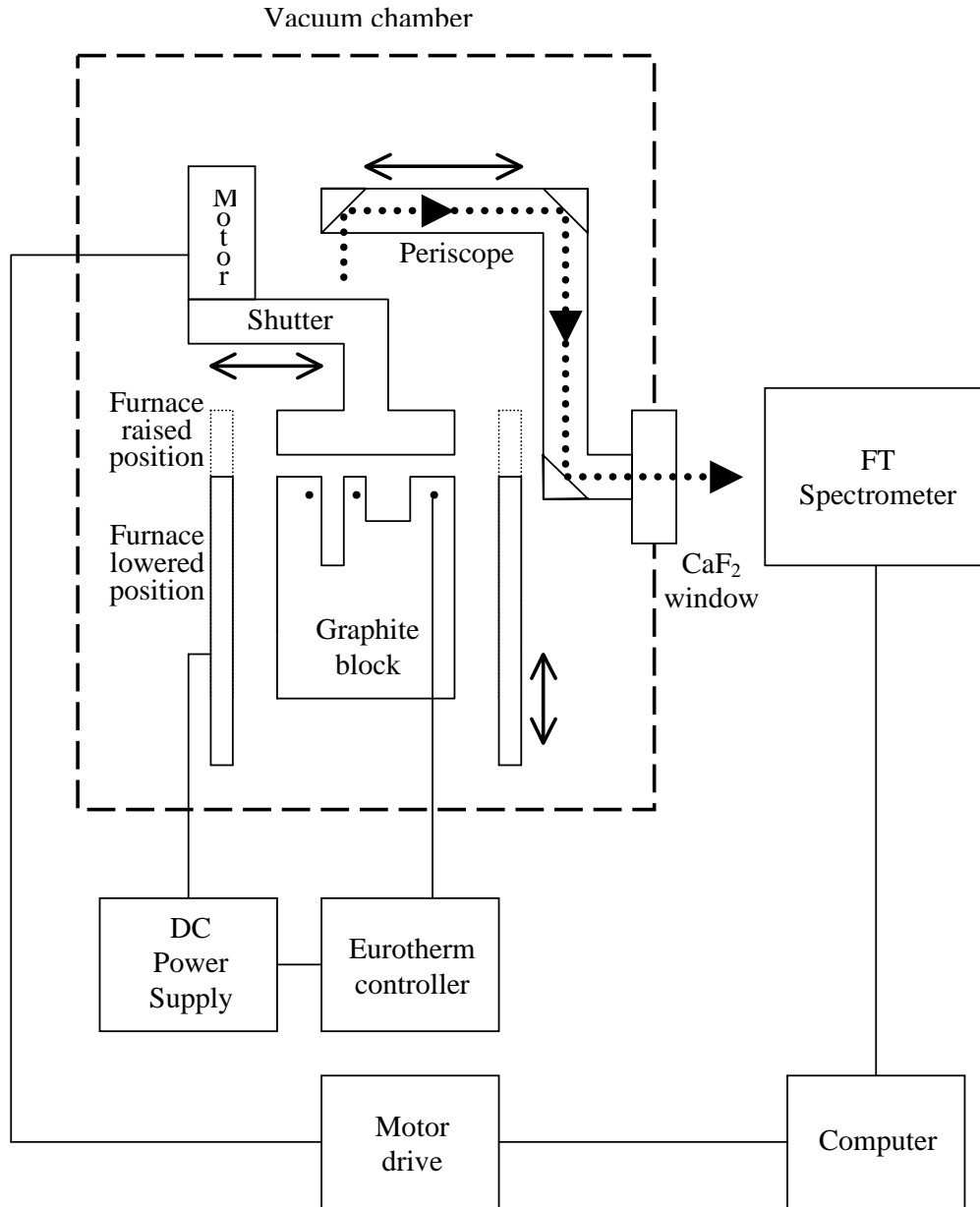


Figure 5 Block diagram of the NPL emissivity measurement apparatus, where three dots show thermocouple positions inside the graphite block.

The apparatus employs an Equinox 55 FT-IR spectrometer supplied by Bruker (UK) Ltd. that has 16-bit data resolution. The instrument has a choice of two beamsplitters,

quartz and Ge/KBr, and three detectors (silicon diode, LN<sub>2</sub>-cooled InSb and MCT) to cover different wavelength ranges. The combinations of the beamsplitters and detectors ensure that the spectrometer can measure radiation over the wavelength range of 0.6 μm to 9.6 μm. The upper limit of 9.6 μm is determined by the cut-off wavelength of the CaF<sub>2</sub> window in the vacuum chamber.

#### 4 Measurements

Before a total emissivity measurement is made, different factors need to be considered to ensure that: (i) the total measurement time  $\Delta t$  is smaller than that of the heat diffusion time from the sample centre to its nearest edge (the thickness or radius of the sample,  $L$ , whichever is smaller) to avoid thermal reflections from its boundaries, *i.e.*  $\Delta t < L^2 \alpha^{-1}$ , and (ii) the measurement speed needs to be controlled so that a sufficiently large dynamic range in measurement signal is possible while also avoiding large drops in the sample surface temperature. For instance, to achieve a temperature drop at the sample surface within 1-2% during an emissivity measurement,  $\Delta t$  needs to lie between  $8.3 \times 10^{-5} t_0$  and  $3.5 \times 10^{-4} t_0$ , as illustrated by figure 2. The criteria (i) and (ii) above set the sample sizes and required total measurement time.

To estimate the total measurement time  $\Delta t$ ,  $t_0$  is calculated with equation (7) for some materials using property data shown in table 1. The calculation shows that, for example, to achieve a 1% decrease in the surface temperature for a measurement on Fecralloy steel at  $T_0 = 1000$  K,  $\Delta t = 22$  s is required (see figure 2 for temperature profile and table 1 for  $t_0$  value). However, to achieve the same 1% drop in the surface temperature for Pyroceram 9606 at  $T_0 = 2000$  K, the measurement needs to be completed within  $\Delta t = 9$  ms. Thus, a much faster measurement speed is required to measure accurately Pyroceram 9606 at  $T_0 = 2000$  K. This shows that the evaluation of  $t_0$  will help to define  $\Delta t$  during which there is a sufficient dynamic range of signal for accurate measurement by the spectrometer. Once  $\Delta t$  is determined and the sample's thermal diffusivity  $\alpha$  is known, in order to ensure that the effect of thermal reflections from its boundaries is minimal the constraint  $L > (\alpha \Delta t)^{1/2}$  must apply.

Table 1  $t_0$  calculation for some materials (with nominal thermal properties collected from various sources)

Material	$T_0$ (K)	$\kappa$ (Wm <sup>-1</sup> K <sup>-1</sup> )	$\rho$ (kgm <sup>-3</sup> )	$C$ (Jkg <sup>-1</sup> K <sup>-1</sup> )	$\epsilon$	$\alpha$ ( $\times 10^{-6}$ m <sup>2</sup> s <sup>-1</sup> )	$t_0$ ( $\times 10^4$ s)
Boron nitride	1000	0.3	2250	1700	0.75	0.784	0.0635
Fecralloy steel	1000	16	7220	460	0.25	4.82	26.4
Tantalum	1000	60	16670	152	0.2	23.7	118
Pyroceram	2000	2.8	2600	1500	0.7	0.718	0.0108
Silicon	2000	124	2330	702	1.0	75.8	0.0986

Tungsten	2000	119	19300	135	0.5	45.7	0.603
----------	------	-----	-------	-----	-----	------	-------

During an emissivity measurement, a baseline (zero) reading is required to determine signal values and for this purpose a few readings are recorded with a white card placed over the vacuum chamber window. After the card is removed and the shutter signal recorded for a few seconds, the furnace is lowered from its raised position (see figure 4) and then the shutter withdraws at speed to expose the target (specimen or blackbody) for measurements. The measured signals peak at about 6  $\mu\text{m}$  and gradually decrease towards shorter and longer wavelengths. A large drop is observed near 4.3  $\mu\text{m}$ , almost certainly due to absorption by laboratory air between the chamber window and FTS detector. The signals also show a slight decrease with time corresponding to the slowly decreasing surface temperature as the sample radiates freely following exposure for measurement.

Having recorded the specimen and blackbody signals, the specimen emissivity can be calculated. At each wavelength the signal-versus-time data can be fitted to the theoretical model to find the signal at time zero, corresponding to the moment immediately before removal of the shutter when the target was isothermal and at a known temperature, as measured by thermocouples. Then the ratio of specimen to blackbody signal at each wavelength gives the respective spectral emissivity value. Using Planck's law, the calculated emissivity value can be adjusted as necessary to compensate for any initial temperature difference between the specimen and blackbody.

A medium-ground FeCrAlloy steel of 1 cm in diameter and 1 cm thick, having low emissivity and moderate effusivity, was chosen for measurement in this study. The radius of the FeCrAlloy sample is slightly smaller than the minimum size dimension set by  $L > (\alpha\Delta t)^{1/2}$ . However, this will not raise a major difficulty in the measurement here because heat transfer at the sample cylindrical surface is much reduced due to it being surrounded by the graphite sample block (figure 5).

Normal spectral emissivity measurements were made on the FeCrAlloy sample at 683 K, 778 K and 1073 K. Signals v. time and wavelength are illustrated in figure 6 for the measurement at 1073 K. Each measurement consists of 200 scans measured with the MCT detector during about 18 s over a wavenumber range of 0 - 5000  $\text{cm}^{-1}$  (*i.e.* wavelength  $\infty$  - 2  $\mu\text{m}$ ) with a resolution of 16  $\text{cm}^{-1}$  (*e.g.* 0.0064  $\mu\text{m}$  resolution at 2  $\mu\text{m}$ , and 0.16  $\mu\text{m}$  resolution at 10  $\mu\text{m}$ ). Each scan took about 90 ms during which the scanning time of the moving mirror in the FTS was about 60 ms and the remaining 30 ms for data transfer and preparation for the next scan.

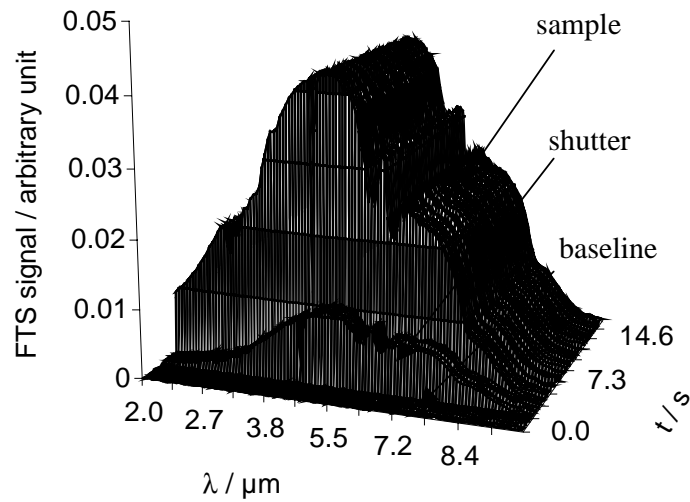


Figure 6 MCT detector signals from Fecralloy sample at 1073 K. The baseline, shutter and sample signals are indicated.

The measured spectral emissivity values are shown in figure 7. No significant change in measured emissivity is observed with respect to temperature, which supports the assumption used in the modelling earlier that temperature related emissivity changes are negligibly small.

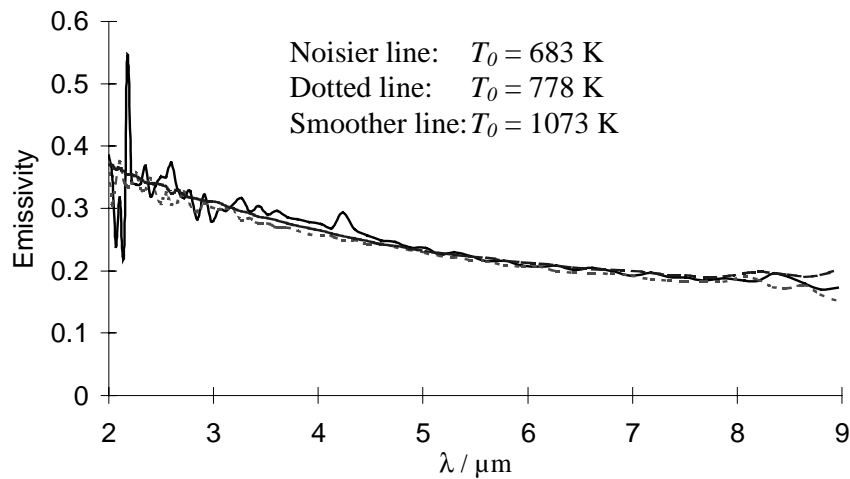


Figure 7 Spectral emissivity measurements on a medium-ground Fecralloy steel at temperatures 683 K, 778 K and 1073 K.

Prior to evaluating hemispherical total emissivity  $\varepsilon$  with equation (7), we need to calculate the specific time  $t_0$  from emissivity measurement. The theoretical modelling in section 2 indicates that  $t_0$  can be calculated from fitting equation (10) to the measured spectral data. Figure 8 shows spectral signals at 2  $\mu\text{m}$ , 3  $\mu\text{m}$  and 4  $\mu\text{m}$  respectively, extracted from the measurement on Fecralloy at 1073 K, with their corresponding best-fit curves each of which produces a value for  $t_0$ . The advantage of this approach to obtain  $t_0$  is that the calculated  $t_0$  values can be compared with each other to ensure consistency of total emissivity estimation with respect to wavelength  $\lambda$ .

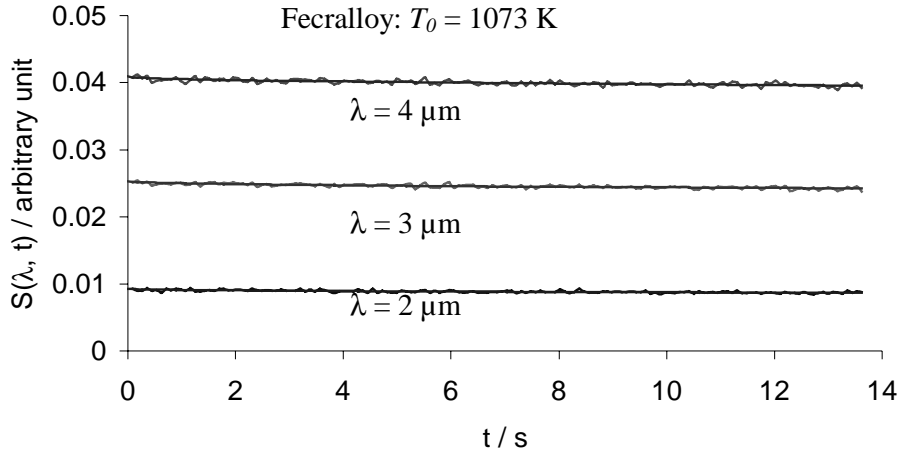


Figure 8 Spectral signals measured from Fecralloy at 1073 K at 2  $\mu\text{m}$ , 3  $\mu\text{m}$  and 4  $\mu\text{m}$ . The smooth lines are their corresponding best-fit curves.

An alternative approach to obtain  $t_0$  is to fit equation (6) to sample surface temperatures calculated from measured radiation signals using Planck's law and the initial surface temperature measured by thermocouples. This alternative approach has two advantages: (i) coefficients in equation (6) are simpler and independent of wavelength of measured signals; and (ii)  $t_0$  can be calculated from surface temperatures evaluated from measured signals at different wavelengths, usually resulting in a better measurement uncertainty in the hemispherical total emissivity estimation.

Figure 9 shows sample surface temperatures calculated from measured radiation signals between 2  $\mu\text{m}$  and 4  $\mu\text{m}$  for the Fecralloy sample at 1073 K. As expected, the transient surface temperatures calculated from the signals at different wavelengths are in agreement. This temperature consistency implies that the spectral emissivity values at those wavelengths were stable with respect to temperature. It also shows that the sample surface temperature decreased from 1073 K to about 1063 K during a measurement time period of about 14 s. Although the surface temperatures has a  $\pm 5$  K variation range and they seem noisy in the expanded scale, the total emissivity value evaluated from them is in agreement, as discussed below.

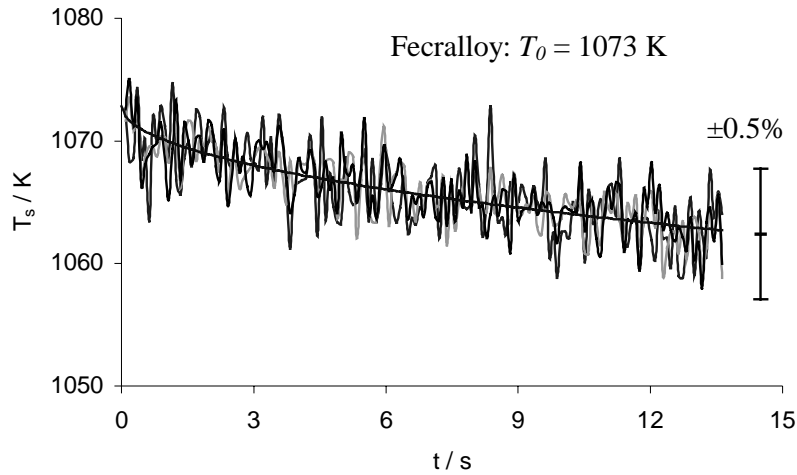


Figure 9 Surface temperatures calculated from three sets of spectral signals measured at 2  $\mu\text{m}$ , 3  $\mu\text{m}$  and 4  $\mu\text{m}$  for Fecralloy at 1073 K °C. The smooth line is the best-fit curve.

Figure 10 shows those evaluated  $\varepsilon$  values for the Fecralloy sample, in comparison with the normal total emissivity  $\varepsilon_n$  value calculated by integration of the measured normal spectral emissivity values between 2  $\mu\text{m}$  and 9  $\mu\text{m}$ . It shows that  $\varepsilon$  values calculated from radiation signals at wavelengths between 2  $\mu\text{m}$  and 4.5  $\mu\text{m}$  are in agreement, with standard deviations from 6% to 9% (error bars in figure 10). For the signals at  $\lambda \geq 5 \mu\text{m}$ , the estimated  $\varepsilon$  values decrease with wavelength. This is probably due to the increasing noise in measurement signals from the background radiation at those wavelengths.

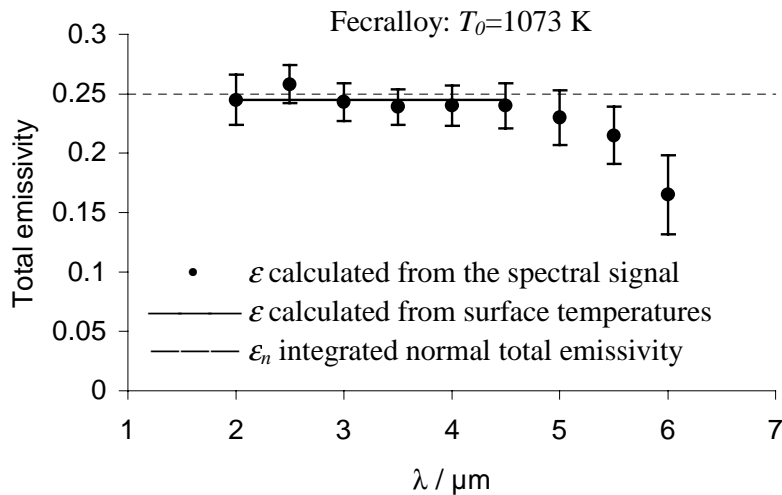


Figure 10 Points: hemispherical total emissivity  $\varepsilon$  from fitting to spectral signals between 2  $\mu\text{m}$  and 4.5  $\mu\text{m}$ . Solid line:  $\varepsilon$  value from surface temperatures

calculated from signals over 2  $\mu\text{m}$  - 4.5  $\mu\text{m}$ . Dotted line: normal total emissivity  $\varepsilon_n$  by integration of spectral emissivity values over 2  $\mu\text{m}$  - 9  $\mu\text{m}$ .

Fitting equation (6) to the surface temperatures calculated from the signals measured at wavelengths between 2  $\mu\text{m}$  and 4.5  $\mu\text{m}$  also gives an  $\varepsilon$  value of 0.245 with a 3% standard deviation (solid line in figure 10). This  $\varepsilon$  value is in good agreement with those calculated from the spectral signals, and about 2% lower than 0.250, which is the normal total emissivity  $\varepsilon_n$  value estimated by integration of the measured spectral emissivity values between 2  $\mu\text{m}$  and 9  $\mu\text{m}$ . Theoretical study shows that  $\varepsilon$  can be up to 10% higher than  $\varepsilon_n$  for polished metals [Siegel and Howell, 1992].

For the measurements at 683 K and 778 K, the low signal-to-noise ratio (SNR) of spectral signals makes the estimated  $\varepsilon$  values vary significantly ( $> 20\%$ ) with large uncertainties. Calculation also shows that radiation from the environment causes about 0.6 % uncertainty in the hemispherical total emissivity estimation at 1073 K, but it increases to 3.9 % for the measurement at 683 K.

## 5. Conclusion

We have described a technique for estimation of hemispherical total emissivity values based on knowing the initial temperature and effusivity of a material, and compared it with total emissivity measurements derived from integration of spectral emissivity measurements. A theoretical model has been developed to study the temperature, radiance and spectral radiation signals from a sample surface during a transient emissivity measurement. Calculations show that the temperature and radiance decrease non-linearly with measurement time, particularly at early time where the change rates can be high for materials of low effusivity and high emissivity. Therefore, measurement speed is important when considering the accuracy of the total emissivity estimation.

The preliminary emissivity measurements on a sample of medium-ground Fecralloy steel show that calculated surface temperatures are consistent at wavelengths between 2  $\mu\text{m}$  and 4.5  $\mu\text{m}$ . Large variation in the total emissivity measured at longer wavelengths is believed to be due to the low SNR caused by the stronger background radiation. The estimated total emissivity obtained by the new approach is in good agreement with that obtained by integration of measured spectral emissivity values.

This is an early look at a possible novel means to obtain an independent check of the total emissivity value that is obtained by the new NPL emissometer. Further investigation of the technique is required to assess its value for a wider range of materials and emissivities.

## Acknowledgement

This work is supported by the DTI NMS Thermal programme (2001-2004) of UK.

## References

1. Y S Touloukian and D P DeWitt (eds.), *Thermal radiative properties – metallic elements and alloys, Thermophysical properties of matter*, **7** (IFI/Plenum, New York – Washington, 1970)
2. Touloukian Y S and DeWitt D P (eds.), *Thermal radiative properties – non-metallic solids, Thermophysical properties of matter*, **8** (IFI/Plenum, New York – Washington, 1972)
3. Ballico M J and Jones T P, *Appl. Spectroscopy* **49**:335 (1995)
4. Werner L, *Metrologia* **32**:531-534 (1995/1996)
5. Clausen S, Morgenstjerne A and Rathmann O, *Appl. Opt.* **35**: 5683 (1996)
6. Redgrove J S, *High Temp. - High Press.* **17**:145 (1985)
7. Zhang B, Redgrove J S and Clark J N, presented on *16<sup>th</sup> European Conference on Thermophysical Properties (ECTP)*, London (2002)
8. Jaeger J C, *Proc. Camb. Philos. Soc.* **46**:634-641 (1950)
9. Siegel R and Howell J R (eds.), *Thermal radiation heat transfer* (Taylor & Francis, Washington, 3<sup>rd</sup> ed., page 122, 1992)

## Appendix

### Surface radiation from a semi-infinite solid

The surface temperature of a semi-infinite sample with surface radiation cooling to an environment at 0 K temperature has been investigated by Jaeger [1950]. In real emissivity measurements, particularly at temperatures near room temperature, heat from the environment to the sample also needs to be considered with radiation heat loss at the sample surface given by equation (2). Considering its initial condition and the heat flow continuity between thermal conduction inside the sample and radiation heat flux from its surface, equation (1) can be solved to give

$$T(x,t)=T_0+T_0 \sum_{n=1}^{\infty} \frac{2^n}{n!} a_n \Gamma\left(\frac{n}{2}+1\right) \left(\frac{t}{t_0}\right)^{\frac{n}{2}} i^n \operatorname{erfc} \frac{x}{\sqrt{4at}} \quad (\text{A1})$$

for  $t > 0$ , where  $\Gamma(y)$  is the Gamma function and  $a_n$  is the  $n^{\text{th}}$  coefficient, given by

$$a_1 = -1.1284 u$$

$$a_2 = 8 u$$

$$a_3 = -72.216 u - 34.481 u^2$$

$$a_4 = 768 u + 1230.7 u^2 + 91.673 u^3$$

$$a_5 = -9243.7 u - 33514 u^2 - 11136 u^3 - 117.07 u^4$$

$$a_6 = 1.2288 * 10^5 u + 8.4872 * 10^5 u^2 + 6.9468 * 10^5 u^3 + 66367 u^4$$

$$a_7 = -1.7748 * 10^6 u - 2.1223 * 10^7 u^2 - 3.0489 * 10^7 u^3 - 9.3686 * 10^6 u^4 - 2.7193 * 10^5 u^5$$

$$a_8 = 2.7525 * 10^7 u + 5.3688 * 10^8 u^2 + 1.4088 * 10^9 u^3 + 8.4912 * 10^8 u^4 + 9.1825 * 10^7 u^5 + 7.2020 * 10^5 u^6$$

and so on, where

$$u = 1 - \frac{T_a^4}{T_0^4}$$

The above derivation shows that, when  $T_0 \gg T_a$ , heat absorbed by the sample surface from the environment can be considered negligible in comparison with heat radiated from the surface. Then  $u=1$  and  $a_n$  become constants.

Surface temperature,  $T_s(t)$  in equation (6) can be derived by setting  $x = 0$  in equation (A1) with use of [Jaeger, 1950]

$$i^n \operatorname{erfc} 0 = \frac{1}{2^n \Gamma\left(\frac{n}{2} + 1\right)}$$

Coefficients  $b_n$  in equation (8) for calculating the radiation heat flux at the sample surface can be calculated to give

$$b_1 = -4.5135 u$$

$$b_2 = 32 u + 15.279 u^2$$

$$b_3 = -288.87 u - 462.90 u^2 - 34.481 u^3$$

$$b_4 = 3072 u + 11138 u^2 + 3701.0 u^3 + 38.908 u^4$$

$$b_5 = -36975 u - 2.5538 * 10^5 u^2 - 2.0903 * 10^5 u^3 - 19970 u^4$$

$$b_6 = 4.9152 * 10^5 u + 5.8776 * 10^6 u^2 + 8.4438 * 10^6 u^3 + 2.5946 * 10^6 u^4 + 75311 u^5$$

$$b_7 = -7.0992 * 10^6 u - 1.3847 * 10^8 u^2 - 3.6335 * 10^8 u^3 - 2.1900 * 10^8 u^4 - 2.3683 * 10^7 u^5 - 1.8575 * 10^5 u^6$$

and so on. The above shows that, when  $T_0 \gg T_a$ ,  $b_n$  become constants.

Coefficients  $d_n$  in equation (10) for calculating spectral radiation signals can be calculated by expanding equation (9) in the form of a Taylor series, to give

$$d_1 = \frac{B}{B-1} A a_1$$

$$d_2 = \frac{B^2 + B}{(B-1)^2} A^2 a_1^2 - \frac{2B}{B-1} A a_1^2 + \frac{B}{B-1} A a_2$$

$$d_3 = \frac{B^3 + 4B^2 + B}{(B-1)^3} A^3 a_1^3 + \frac{2B^2 - 6B}{(B-1)^2} A^2 a_1^3 + \frac{6B}{B-1} A a_1^3 + \frac{3B^2 + 3B}{(B-1)^2} A^2 a_1 a_2$$

$$- \frac{6B}{B-1} A a_1 a_2 + \frac{B}{B-1} A a_3$$

$$d_4 = \frac{B^4 + 11B^3 + 11B^2 + B}{(B-1)^4} A^4 a_1^4 - \frac{4B^3 + 32B^2 + 7B}{(B-1)^3} A^3 a_1^4 - \frac{4B^2 - 36B}{(B-1)^2} A^2 a_1^4$$

$$+ \frac{6B^3 + 24B^2 + 6B}{(B-1)^3} A^3 a_1^2 a_2 - \frac{12B^2 + 36B}{(B-1)^2} A^2 a_1^2 a_2 + \frac{36B}{B-1} A a_1^2 a_2$$

$$+ \frac{3B^2 + 3B}{(B-1)^2} A^2 a_2^2 - \frac{6B}{B-1} A a_2^2 + \frac{4B^2 + 4B}{(B-1)^2} A^2 a_1 a_3$$

$$- \frac{8B}{B-1} A a_1 a_3 + \frac{B}{B-1} A a_4$$

and so on, where

$$A = \frac{C_2}{\lambda T_0} \quad \text{and} \quad B = e^{\frac{C_2}{\lambda T_0}}$$